Journal of Materials Chemistry C

ROYAL SOCIETY OF CHEMISTRY

PAPER

View Article Online
View Journal | View Issue

Cite this: J. Mater. Chem. C, 2025, 13, 20259

New cationic fluorescent dyes for optical sensing of chloride

Karl L. Sterz, Torsten Mayr * and Sergey M. Borisov *

Lucigenin (10,10′-dimethyl-[9,9′-biacridine]-10,10′-diium nitrate) is a fluorescent compound known for more than a century for its chloride sensitivity, but further research since then has not yielded definitive improvements or extensive structure–property relations. Chloride indicators that absorb and emit at longer wavelengths are highly desirable to minimize interference through scattering, autofluorescence of optical components and samples, particularly when measuring in biological probes. Herein, the synthesis and spectral properties of new π-extended lucigenin analogs are reported. *N*-Methyl benzo[*b*]acridinium (**1**) and two-fold-charged dyes incorporating the benzo[*b*]acridinium backbone (**2**, **3**) are not emissive, and a fluorescent π-extended derivative incorporating a fluorene structure (**4**) does not show a sizeable response to chloride ($K_{SV\,NaCl}$ = 0.8 M^{-1}). A novel dicationic perylene analog, 3,9-dimethylbenzo[1,2,3-*de*:4,5,6-*d*′*e*′]diquinoline-3,9-diium (**6**), shows typical spectral characteristics of perylene and fluorescence quantum yield close to unity but also a strong fluorescence response to chloride ($K_{SV\,NaCl}$ = 160 M^{-1}). Compared to lucigenin (ε = 7.5 × 10^3 M^{-1} cm^{-1} at 433 nm, Φ = 52%), **6** shows much higher (~5-fold) brightness in the visible spectral range (ε = 2.2 × 10^4 M^{-1} cm^{-1} at 455 nm, Φ = 97%). Finally, a hybrid of acridinium and quinolinium, 10-methyl-9-(1-methylquinolin-1-ium-5-yl)acridin-10-ium (**5**), is characterized by spectral properties, brightness (ε = 5.1 × 10^3 M^{-1} cm^{-1} at 426 nm, Φ = 83%) and chloride response ($K_{SV\,NaCl}$ = 145 M^{-1}) which are similar to lucigenin, but without detectable crosstalk to common anions such as nitrate and sulfate ($K_{SV\,NaNO_3} \approx 0$, $K_{SV\,Na_2SO_4} \approx 0$). In addition, the indicator features extraordinarily long fluorescence lifetime (τ = 24.5 ns) that also decreases in presence of chloride, which suggests high potential of the new dye as a water-soluble probe for chloride mapping by fluorescence lifetime imaging methods. The dye can also be photoimmobilized into partly hydrolyzed poly(acrylonitrile) providing a sensor material with similar characteristics to lucigenin, but without crosstalk to nitrate and sulfate.

Received 6th June 2025,
Accepted 1st September 2025

DOI: 10.1039/d5tc02192h

rsc.li/materials-c

1. Introduction

The luminescence quenching mechanism of lucigenin (L^{2+}, Fig. 1) by chloride was already investigated five decades ago.[1] It was found that the ionization potential of the analyte correlates with the quenching efficiency which likely occurs through formation of a charge transfer complex of the following nature:[1]

$$L^{2+} + h\nu \rightarrow (L^{2+})^*$$

$$(L^{2+})^* + Cl^- \rightarrow (L^{\bullet+}Cl^{\bullet})$$

$$(L^{\bullet+}Cl^{\bullet}) \rightarrow L^{2+} + Cl^-$$

Institute of Analytical Chemistry and Food Chemistry, Graz University of Technology, Stremayrgasse 9, 8010, Graz, Austria. E-mail: torsten.mayr@tugraz.at, sergey.borisov@tugraz.at

Lucigenin (L^{2+}) is electronically excited by electromagnetic radiation, and the excited compound interacts, mainly diffusion controlled, with chloride. A charge-transfer process yields a pair of de-excited radicals. Through another charge transfer, the initial species are regenerated. Luminescence quenching of lucigenin occurs most efficiently through charged species (I^-, Br^-, Cl^-, acetate),[2,3] but electronic charges are no prerequisite for quenchers, since quenching by DMSO and 1,3-bis(tris(hydroxymethyl)methylamino)propane also has been reported.[2] Negative electronic charges on quenchers are assumed to decrease the activation energy for formation of the respective charge-transfer complex. Luminescence quenching by formation of charge-transfer complexes is also suggested for quinolinium-type dyes, emphasizing the similarity between acridinium and quinolinium-type dyes.[4]

Lucigenin, a compound first reported in 1906,[5] remains widely used in analytical chemistry,[6,7] especially for optical chloride measurements[8,9] due to acceptable photophysical properties (absorption maxima at 369 nm and 430 nm,

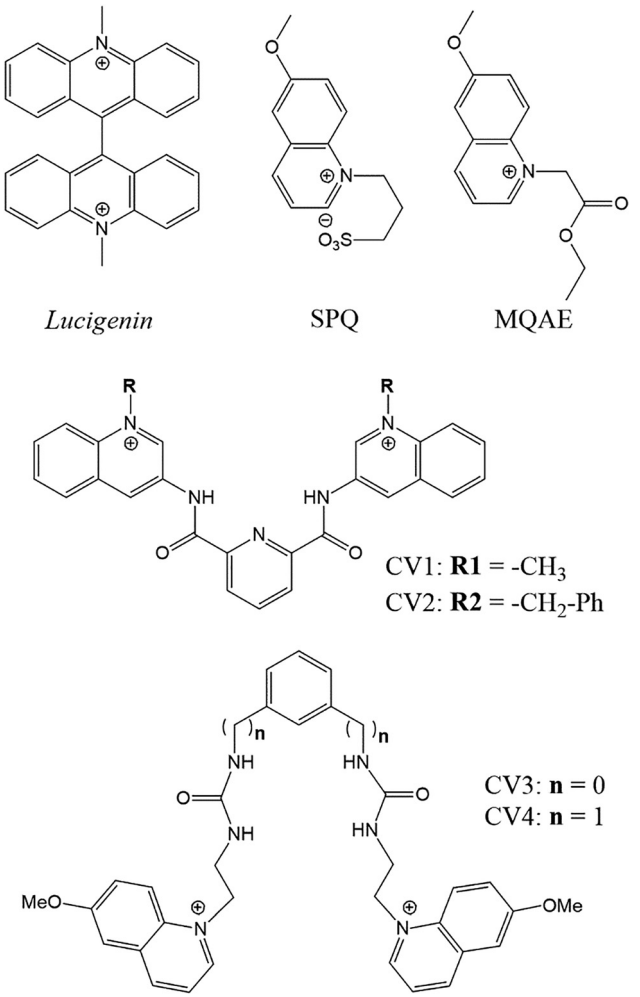

Fig. 1 Examples of reported chloride-sensitive fluorescent dyes, including SPQ,[13,14,25] MQAE,[13,14] CV1-2[26,27] and CV3-4.[28]

emission maximum at 508 nm, good fluorescence brightness) and high chloride sensitivity ($K_{SV\,Chloride}$ = 390 M^{-1}).[3] Apart from applications of lucigenin in sensing materials,[10–12] past research was focused on elucidation of the structure–property relation of lucigenin and the synthesis of new indicators with improved properties.[3,13–16] Although none of the new dyes (Tables S1 and S2) significantly outperformed lucigenin, some, like quinolinium dyes, proved more suitable for specialized applications, like chloride measurements in living cells.[3,13,14,17–24]

In case of acridinium dyes, electronically neutral substitutions are mostly introduced at the 9-position, with aliphatic, π-donor and π-acceptor substitutions being reported in the literature[3,15] (Tables S1 and S2). π-Acceptors generally induce a bathochromic shift,[3,15] for instance in 9-(methoxycarbonyl)-*N*-methylacridinium ($\lambda_{abs\,max}$ = 424 nm, $\lambda_{em\,max}$ = 520 nm) compared to *N*-methyl acridinium ($\lambda_{abs\,max}$ = 415 nm, $\lambda_{em\,max}$ = 492 nm).[3,15] The molar absorption coefficients (ε) of 9-substituted acridinium dyes are usually about half that of lucigenin, but the quantum yield (Φ) may be higher than that of lucigenin.[3,15] The introduction of aliphatic hydrocarbons or π-donors at the 9-position drastically reduces the chloride sensitivity, yielding dyes with 0.3–2.3% of the $K_{SV\,Chloride}$ of lucigenin.[3,15] π-Acceptor substitution at the 9-position leads to dyes with generally higher $K_{SV\,Chloride}$, (21–58% of the $K_{SV\,Chloride}$ of lucigenin).[3,15] This demonstrates that the chloride sensitivity is a parameter which is highly sensitive towards structural changes.[3,15]

Compared to acridinium, quinolinium dyes show strongly blue-shifted absorption and emission maxima.[3,13,14,28] Also, *N*-aliphatic acridinium compounds with π-acceptor substituents at the 9-position commonly reach higher $K_{SV\,Chloride}$ values than most *N*-aliphatic quinolinium dyes[3,13–16,25] (Tables S1 and S2). 6-Methoxy-*N*-(3-sulfopropyl)quinolinium (SPQ)[3,13,14,21,23] (Fig. 1) is the most popular indicator of this group, particularly in intracellular applications.[16,21] It is characterized by absorption and emission maxima of 350 and 440 nm, respectively,[13,14] Φ of 60% in water,[14] and the $K_{SV\,Chloride}$ value of ~30% that of lucigenin.[3,13,14] The higher selectivity of SPQ towards chloride often justifies its preference over lucigenin.[9,13,16] Investigation of the structure–property relationships of the quinolinium dyes shows that chloride sensitivity strongly depends on the chemistry and position of the substituents.[13,14,16] For instance, a spectrally similar SPQ analogue, bearing the methoxy substituent at the 7-position, instead of the 6-position, showed only about 7% the $K_{SV\,Chloride}$ of SPQ.[14] Generally, substitution at the 6-position with methyl- and methoxy-groups increases halide sensitivity, whereas the opposite effect is observed for chloro-, bromo- and benzyl-substituents in the molecule.[13,14,16,25] Substitution at the 8-position strongly decreases chloride sensitivity but leads to pronounced bathochromic shift of the dye emission (~50 nm).[16] Different substituents at the nitrogen atom change the properties of quinolinium dyes comparatively little.[13,14,16,25]

An approach to develop more selective chloride-sensitive dyes is to use cavity-forming luminescent compounds **CV1–4** (Fig. 1).[26–28] The compounds are optimized in terms of intramolecular distances and availability of polarized hydrogen bonds, forming a cavity of a specific size. Through chelation, a specific anion can be incorporated, which in turn may quench the fluorescence of the π-conjugated part. Compounds of this type may also be described as chloride-receptors. Chloride-sensitive receptors include bisquinolinium pyridine dicarboxamide type dyes,[26,27] but metal-based receptors[29] are also known. Generally, the quenching behavior of **CV1–4** is unlike typical quinolinium dyes: the quenching by bromide and iodide tends to be comparable or even weaker than for chloride, although the heavier halogenides generally quench the luminescence of quinolinium dyes stronger because of the heavy atom effect.[3,16] Unfortunately, the cavity-forming chloride indicators usually show strong pH dependency and can be poorly soluble in water.[26,27,29]

Some proteins are also known to possess chloride sensitivity.[30–33] Upon targeted mutation, these properties were shown to be tunable.[30,31,33] These fluorescent proteins have attractive spectral properties, but also many drawbacks including strong pH dependency, low selectivity, a low fraction of dynamic quenching and generally much lower chloride sensitivity compared to lucigenin.

Despite limitations of the indicators mentioned above, some have been widely used in numerous environmental and biological analyses. In living organisms, chloride is the most abundant anion for regulatory purposes, and it is responsible for control of membrane potential, cell volume and charge balance, as well as pH and likely intracellular traffic.[13,22] Several diseases and health conditions are known, for instance cystic fibrosis[13,25] and cholera,[13] which can cause changes in chloride concentrations within a patient's body or fluids,[13,30] emphasizing the need for solid chloride analysis. Quinolinium dyes,[13,18] specifically SPQ[17,21,24] and *N*-ethoxycarbonylmethyl-6-methoxyquinolinium bromide (MQAE),[14,19,24] are commonly used to measure the chloride concentration in diverse biological systems, providing vectors towards disease diagnostics[13] and research[18,19] alike. They are often entrapped into membrane vesicles and liposomes prior to deployment,[13,14,17,21] providing an avenue for quantitative analysis of transmembrane chloride transport[17,25] and intracellular chloride content.[13,14] In case of lucigenin, its immobilization into (nano)particles may further be required to suppress cross-sensitivity in biological systems.[34,35] Lucigenin has further found use in optical sensor technology, utilizing dual lifetime referencing (DLR) techniques[10] to assess chloride contamination in concrete[12] and the seawater salinity *via* chloride concentration.[11] Chloride quantification in reinforced concrete is crucial, as the embedded iron rebar is susceptible to chloride-induced corrosion, rendering infrastructure highly prone towards collapse.[12] Seawater salinity analysis can provide vital insights into ocean circulations and analysis of marine life habitats.[11]

In this work we synthesized new cationic dyes, either fully planar or consisting of two planar fragments connected together *via* a single bond. Investigation of their photophysical properties and fluorescence response to chloride revealed two new promising chloride indicators that overcome some of the limitations of lucigenin.

2. Experimental

2.1. Materials and synthesis

Sources of commercially available chemicals, synthesis of intermediates and the dyes, NMR spectra, mass spectrometry data are covered in the SI.

2.1.1. Preparation of sensing foils. 65 mg of the hydrolysed PAN polymer (for the detailed procedure see Section S2.2 of SI) were dissolved in 580 mg dimethyl sulfoxide (≥99.5% for synthesis, Roth) under stirring and the solution was knife-coated onto a poly(ethylene terephthalate foil) (PET, 175 μm thickness, Alcan Packaging Singen GmbH), which was roughened using abrasive paper. After evaporation of the solvent at room temperature, either a 3.5×10^{-1} mg mL^{-1} aqueous solution of lucigenin or a 3.2×10^{-1} mg mL^{-1} aqueous solution of 10-methyl-9-(1-methylquinolin-1-ium-5-yl)acridin-10-ium dinitrate **5** was applied to the film and irradiated with the UV lamp (Herolab GmbH, type: NU-8, 8 W) at λ = 365 nm for 8 h. Afterwards, the sensor foil was washed extensively with demineralized water and a 1 M sodium nitrate solution.

Dye-loaded Nafion foils were made by applying a commercial 5 wt% Nafion 117 solution (Merck) to a PET-SiO_x substrate foil (175 μm thickness) using a knife-coating device. The solvent was allowed to evaporate for 24 h and the dry foil was submerged in a 5×10^{-2} mg mL^{-1} aqueous solution of the respective dye and kept for 24 h. Afterwards, the foil was extensively rinsed with demineralized water, a saturated sodium chloride solution, a 1 M sodium nitrate solution and finally demineralized water.

2.2. Characterization of optical properties

The photophysical properties were studied in demineralized water. Absorption spectra were recorded on a Cary 60 UV-VIS Spectrophotometer (Agilent). Emission spectra were recorded in demineralized water on a Jobin Yvon Fluorolog 3 spectrometer from Horiba equipped with a R2658 photomultiplier from Hamamatsu. The Stern–Volmer constants were calculated from the intensities of the emission spectrum maxima. The fluorescence decay times were measured with time correlated single photon counting (TCSPC) technique on the same device equipped with Delta hub module (Horiba) using a 453 nm laser diode "NanoLED" (Horiba) for the excitation and DAS-6 Analysis software for data analysis. Solution measurements were conducted in a standard quartz glass cuvette (Hellma® Analytics, 10 × 10 mm path length, 3.500 mL cell volume). The absolute quantum yield was determined using an integrating sphere setup (Horiba) and all measurements were conducted with the dye dissolved in demineralized water. The titrations were conducted with manual Eppendorf pipettes (10–100 μL, 100–1000 μL) from LLG Labware. In case of the sensor materials, the foils were cut and fixed in a home-made flow-through cell to be read-out with the Fluorolog 3 spectrometer. The error of the Stern–Volmer data points was calculated using error propagation. In case of quenching by sodium bromide and sodium iodide, the modified equation $I_0/I = 1 + (K_{SV} + K_{stat})\cdot[Q] + K_{SV}\cdot K_{stat}\cdot[Q]^2$ was used.[9] It describes a dynamic (K_{SV}) and a static (K_{stat}) contribution on intensity quenching at a quencher concentration ([Q]).

3. Results and discussion

Fig. 2 provides an overview of lucigenin analogs investigated. These can be divided into several categories. The first comprises *N*-methyl-benzo[*b*]acridinium dyes that include the simplest representative **1** and dyes **2** and **3** where benzo[*b*]acridinium unit is connected to acridinium (**2**) or quinolinium (**3**) part. The second group (dyes **4** and **5**) includes closer analogs of lucigenin. Finally, the last groups include rigidized dyes **6–8** which are structurally very different from lucigenin and also show very different spectral characteristics. To the best of our knowledge, such positively charged polycyclic aromatic nitrogen-containing heterocycles (*N*-PAHs) have not been yet investigated for potential chloride-sensing capabilities.

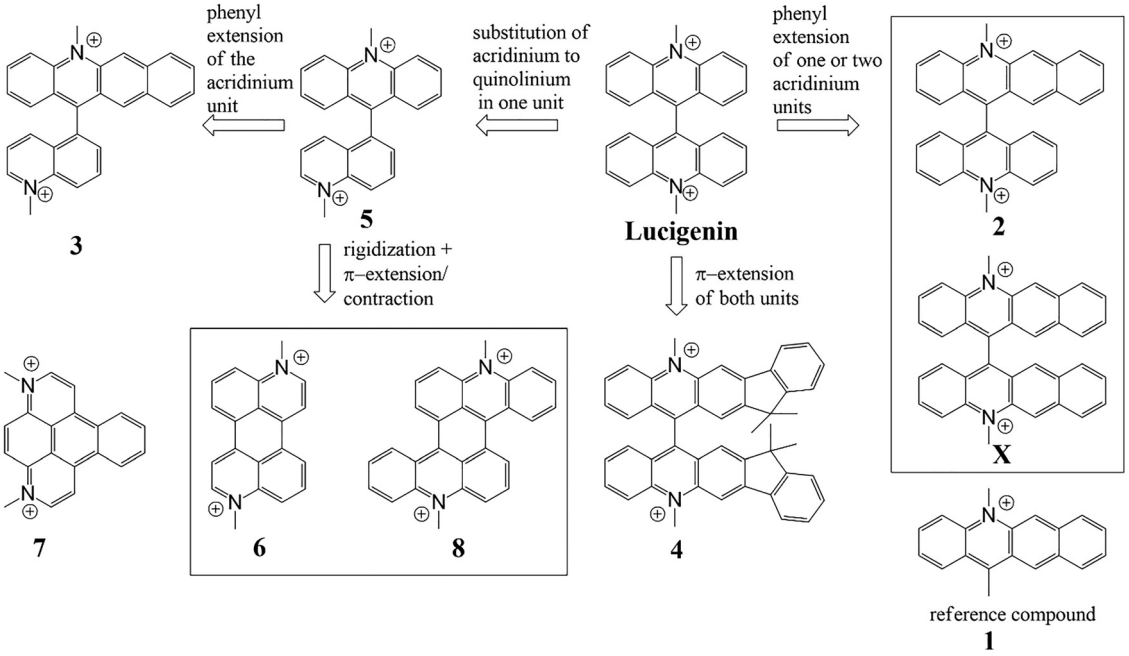

Fig. 2 Chemical structures of lucigenin and the new dyes.

3.1. New π-extended analogs of lucigenin (2–4)

3.1.1. Synthesis. A π-extended analog of lucigenin, 5,5′-dimethyl-[12,12′-bibenzo[*b*]acridine]-5,5′-diium (**X**), was an obvious target of our study. Unfortunately, the synthesis proved challenging. Attempts to prepare this compound by adapting synthetic procedures known for lucigenin, such as condensation with hydrochloric acid and zinc,[36] Suzuki coupling or McMurry reaction, yielded no product or only trace amounts (Fig. S1 and S2). A Miyaura–Suzuki reaction, using 12-bromobenzo[*b*]acridine, yielded some of the pinacol ester, as detected with APCI-mass spectrometry, however the compound readily decomposed during workup under ambient conditions.

Thus, in order to get insights on the effect of π-extension we prepared the simplest representative 5,12-dimethylbenzo[*b*]-acridin-5-ium (**1**), 5-methyl-12-(10-methylacridin-10-ium-9-yl)-benzo[*b*]acridin-5-ium (**2**), which is essentially lucigenin extended by one phenyl ring, and 5-methyl-12-(1-methylquinolin-1-ium-5-yl)benzo[*b*]acridin-5-ium (**3**). Compound **1** was obtained *via* Grignard reaction of 5-methylbenzo[*b*]acridin-12(5*H*)-one with solution of methyl magnesium bromide in diethyl ether. After the reaction, methanesulfonic acid was added to facilitate elimination and the compound was repeatedly washed with diethyl ether. The methanesulfonate of **1** is well-soluble in demineralized water and dichloromethane. In contrast, the aqueous solubility of the nitrate form obtained *via* precipitation with KPF_6, and subsequent ion exchange was poor. Compounds **2** and **3** were synthesized *via* Suzuki coupling followed by methylation. To the best of our knowledge, compounds **2** and **3** represent the first reported two-fold-charged water-soluble *N*-methyl benzo[*b*]acridinium dyes. After alkylation, **2** and **3** are readily purified by precipitation with KPF_6 and subsequent ion exchange to the water-soluble nitrate form.

5,5′,7,7′-Hexamethyl-7*H*,7′*H*-[13,13′-biindeno-[1,2-*b*]acridine]-5,5′-diium (**4**) features another pattern of π-extension. The synthesis was done analogously to lucigenin, *via* treatment of the extended *N*-methyl acridone, 5,7,7-trimethyl-5*H*-indeno[1,2-*b*]-acridin-13(7*H*)-one, with hydrochloric acid and zinc. Unfortunately, the reaction was accompanied by the formation of monomeric by-product which in our hands was impossible to remove during chromatographic purification or suppress through changes in the reaction conditions (Fig. S24–S26, S49–S51 and S58–S61).

3.1.2. Optical properties. Fig. 3 shows that the most intense absorption band of dyes **1–3** is bathochromically shifted compared to lucigenin (λ_{max} = 397, 407, 411 and 368 nm for **1**, **2**, **3** and lucigenin, respectively). This band is attributed to transitions localized on the benzo[*b*]acridinium part. Compound **2**, which contains both acridinium and benzo[*b*]acridinium parts, additionally shows a less intense absorption band with the maxima (369 nm) virtually identical to that of lucigenin. This absorption is attributed to the acridinium chromophore. The molar absorption coefficient ε at this wavelength is 1.6 × 10^4 M^{-1} cm^{-1} (Fig. S93), which is approximately half of the value obtained for lucigenin ($\varepsilon = 2.9 \times 10^4$ M^{-1} cm^{-1} at 369 nm, Fig. S92) that bears two acridinium moieties. The absorption of the benzo-[*b*]acridinium part is more efficient ($\varepsilon = 2.3 \times 10^4$ M^{-1} cm^{-1} at 411 nm, Fig. S93) and is similar to the value obtained for the benzo[*b*]acridinium–quinolinium hybrid **3** ($\varepsilon = 2.7 \times 10^4$ M^{-1} cm^{-1} at 407 nm, Fig. deS94). Interestingly, compounds **1–3** also feature an additional significantly less intense and very broad absorption band at longer wavelengths (450–700 nm). Although lucigenin also exhibits low energy absorption bands ($\lambda_{abs\,max}$ = 430, 455 nm) they are much narrower.

Investigation of potential emissive properties of **1–3** revealed no luminescence in the visible part of the electromagnetic

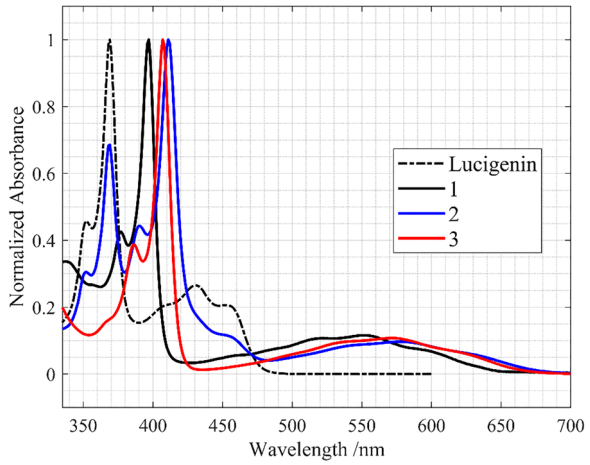

Fig. 3 Absorption spectra of lucigenin, **2**, **3** (all as nitrate form) and **1** (as methanesulfonate form) dissolved in demineralized water.

spectrum upon excitation in any of the absorption bands. This demonstrates how efficiently the *N*-methyl benzo[*b*]acridinium moiety suppresses the emission and suggests that the attempted compound 5,5′-dimethyl-[12,12′-bibenzo[*b*]acridine]-5,5′-diium (**X**) is very unlikely to be a desirable target.

The absorption and emission spectra of **4** (in the mixture with the by-product) are very similar to those of lucigenin but are shifted bathochromically by ∼20 nm and an additional band is observed at λ_{max} = 410 nm (Fig. S58). The fluorescence quantum yield (Φ ∼ 28%) and the decay time (τ ∼18.5 ns, Fig. S100) representing only a rough estimation due to the presence of by-product, also indicate its strong similarity to lucigenin. Strikingly **4** shows only very minor sensitivity towards sodium chloride ($K_{SV\,NaCl}$ = 0.8 ± 0 M^{-1}, Fig. S69) which is in stark contrast to lucigenin ($K_{SV\,NaCl}$ = 360 ± 3 M^{-1}, Fig. S64). Nevertheless, the emission of **4** is quenched by sodium bromide ($K_{SV\,NaBr}$ = 125 ± 6 M^{-1}, $K_{stat\,NaBr}$ = 8 ± 2 M^{-1}, Fig. S70) and sodium iodide ($K_{SV\,NaI}$ = 244 ± 21 M^{-1}, $K_{stat\,NaI}$ = 41± 10 M^{-1}, Fig. S71), albeit at lower magnitude than for lucigenin ($K_{SV\,NaBr}$ = 465 ± 13 M^{-1}, $K_{stat\,NaBr}$ = 6 ± 2 M^{-1}, $K_{SV\,NaI}$ = 452 ± 14 M^{-1}, $K_{stat\,NaI}$ = 50 ± 6 M^{-1}, Fig. S65 and S66). For the heavier halides we observe some contribution of the static quenching (K_{stat}) of similar magnitude as for lucigenin, underlining the structural similarity of the two compounds. Some contribution of the static quenching, particularly in case of iodide, is in line with literature data on lucigenin.[15] The reason for the virtual absence of sensitivity towards chloride in **4** is likely the increased π-electron density due to the introduction of the fluorene moiety which hinders the formation of the desired charge-transfer complex with the quencher. This would imply that a compound may be rendered almost completely chloride-insensitive following these relatively minor structural modifications.

3.2. *N*-Methylquinolinium lucigenin analog 5

3.2.1. Synthesis. Since benzo[*b*]acridinium–quinolinium hybrid **3** was found to be non-emissive, we turned our attention to a closer lucigenin analogue, 10-methyl-9-(1-methylquinolin-1-ium-5-yl)acridin-10-ium (**5**). This compound was synthesized from commercially available precursors in only 2 steps: Suzuki coupling and subsequent methylation of 9-(quinoline-5-yl)-acridine with good yields (∼60% in two stages).

3.2.2. Optical properties. Fig. 4a shows that the absorption and emission spectra of **5** are extremely similar to those of lucigenin and only a very small hypsochromic shift (∼4 nm) is observed compared to the parent compound. As expected, the molar absorption coefficients for the bands in the UV and visible parts of the electromagnetic spectrum (ε = 1.8 × 10^4 and 5.1 × 10^3 M^{-1} cm^{-1} at 366 and 426 nm, respectively, Fig. S95) are about 50% of the lucigenin values. Somewhat surprisingly, **5** shows a significantly higher fluorescence quantum yield (Φ = 83 ± 1%) than lucigenin (Φ = 52 ± 8%). The luminescence brightness (defined as $\varepsilon{\cdot}\Phi$) is thus comparable to lucigenin. The fluorescence lifetime of **5** was measured to be 24.5 ± 0.1 ns (Fig. S101) and is thus significantly higher than that of lucigenin (τ = 19.9 ± 0.1 ns, Fig. S99).

The emission of **5** does not display noticeable sensitivity towards $NaNO_3$ or Na_2SO_4 in the investigated range of 0–1 M (Fig. 4b and Fig. S72, S73), contrary to lucigenin ($K_{SV\,Na_2SO_4}$ = 7.5 ± 0.2 M^{-1}, $K_{SV\,NaNO_3}$ = 0.6 ± 0 M^{-1}, Fig. S62, S63). On the other hand, **5** remains sensitive to chloride ($K_{SV\,NaCl}$ = 145 ± 3 M^{-1}, Fig. S74), as the K_{SV} value is ∼40% that of lucigenin

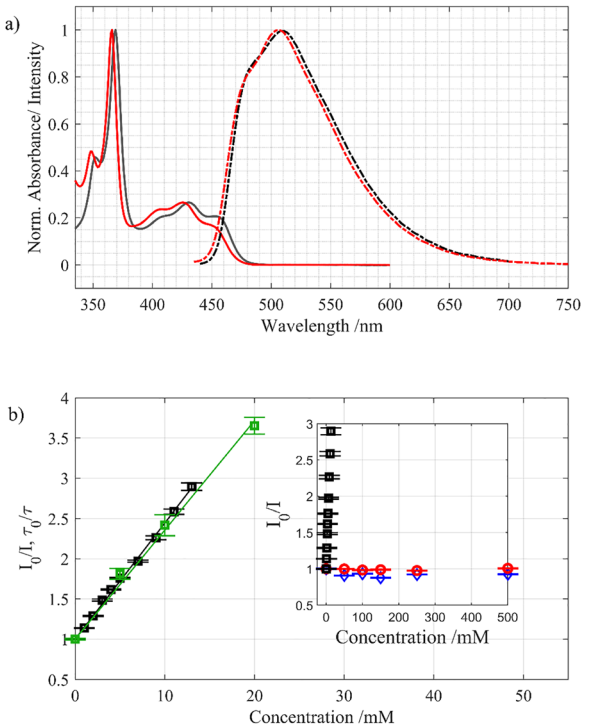

Fig. 4 Spectral and chloride-sensing properties of **5**. (a) Absorption (solid lines) and emission (dashed-dotted lines) spectra of lucigenin (black) and **5** (red) in the nitrate form dissolved in demineralized water (λ_{exc} 420 nm for both dyes). (b) response of fluorescence intensity of **5** (λ_{exc} = 420 nm, λ_{em} = 510 nm) to chloride (black squares), nitrate (red circles) and sulfate (blue diamonds) in the nitrate form in demineralized water. Green squares show the response of the fluorescence decay time to chloride.

($K_{SV\,NaCl}$ = 360 ± 3 M^{-1}, Fig. S64). The chloride sensitivity of **5** is thus well comparable to that of the commonly used SPQ dye.[3,13,14,16,17] Notably, when compared to SPQ, **5** shows much more attractive spectral properties with significantly longer wavelength of absorption and emission, higher molar absorption coefficients and quantum yields. Regarding bromide and iodide, **5** shows slightly more efficient quenching ($K_{SV\,NaBr}$ = 558 ± 2 M^{-1}, $K_{stat\,NaBr}$ = 2.6 ± 0.3 M^{-1}, $K_{SV\,NaI}$ = 656 ± 17 M^{-1}, $K_{stat\,NaI}$ = 21 ± 2 M^{-1}, Fig. S75, S76) compared to lucigenin ($K_{SV\,NaBr}$ = 465 ± 13 M^{-1}, $K_{stat\,NaBr}$ = 6 ± 2 M^{-1}, $K_{SV\,NaI}$ = 452 ± 14 M^{-1}, $K_{stat\,NaI}$ = 50 ± 6 M^{-1}, Fig. S65, S66). Interestingly, the static quenching by the heavier halides appears to be less efficient for **5** than for lucigenin.

Fig. 4b also demonstrates strong dependency of the fluorescence decay time of **5** on chloride concentration. The Stern–Volmer constants are very similar regarding the decay time (K_{SV} = 136 ± 6 M^{-1}) and the intensity ($K_{SV\,NaCl}$ = 145 ± 3 M^{-1}) which confirms the dynamic nature of the quenching process. Considering the extraordinary long fluorescence lifetime of **5**, its attractive photo-physical properties and synthetic accessibility, we expect that it may become a viable probe for chloride imaging in biological systems with help of fluorescence lifetime imaging (FLIM) technique.

3.3. Planar polycyclic dyes 6–8

3.3.1. Synthesis. A perylene analog, 3,9-dimethylbenzo-[1,2,3-*de*:4,5,6-*d′e′*]diquinoline-3,9-diium (**6**) and its isomer 3,6-dimethyldibenzo[*f*,*lmn*][2,9]phenanthroline-3,6-diium (**7**) (Fig. 2) were prepared by methylating the corresponding planar intermediates. These electronically neutral planar intermediates of the compounds **6** and **7** were prepared *via* photolytical and thermal cyclization, respectively, described in literature[37] followed by saponification and decarboxylation (see SI for more details). The π-extended analog of **6**, 8,16-dimethylbenzo[1,2,3-*kl*:4,5,6-*k′l′*]diacridine-8,16-diium (**8**) was obtained *via* methylation of the planar intermediate, benzo[1,2,3-*kl*:4,5,6-*k′l′*]diacridine. This was obtained through a Buchwald–Hartwig coupling reaction, yielding 1,5-bis(phenylamino)-9,10-anthracenedione followed by planarization occurring through water elimination in hot triflic acid.

3.3.2. Optical properties. The absorption and emission spectra of **6**, **7** and **8** are shown in Fig. 5. Compound **6** shows three well-resolved absorption/emission bands in the visible part of the spectrum. The spectral properties are thus extremely similar to that of perylene.[38] Analogously to perylene, the absorption and emission spectra overlap significantly, and the Stokes shift is rather small (8 nm). However, this poses no practical challenge since excitation in the second band, located at 428 nm, can be performed. At this wavelength the molar absorption coefficient was determined to be 1.6 × 10^4 M^{-1} cm^{-1} (Fig. S96) which is about 2-fold the value of lucigenin (ε = 7.5 × 10^3 M^{-1} cm^{-1} at 433 nm, Fig. S92). For **6** the value is even higher at 455 nm (ε = 2.2 × 10^4 M^{-1} cm^{-1}, Fig. S96). Compound **6** shows extremely strong fluorescence with quantum yield close to unity (Φ = 97 ± 8%), which is however not unexpected due to its structural similarity to perylene. Therefore, compared to lucigenin, compound **6** shows 4 to 5-fold enhancement of fluorescence

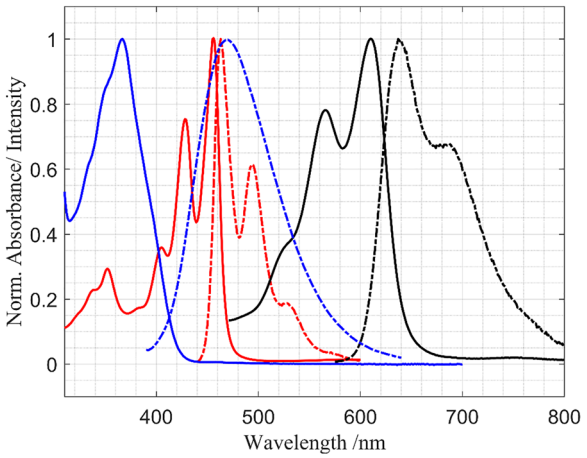

Fig. 5 Absorption (solid lines) and emission (dashed-dotted lines) of **6** (red), **7** (blue) and **8** (black) as $[NO_3]^-$ salts dissolved in demineralized water. The excitation wavelengths are 420, 360 and 525 nm for **6**, **7** and **8**, respectively.

brightness when excitation is performed with visible light. Finally, **6** is characterized by a fluorescence decay time similar to other perylenes (5.5 ns, Fig. S102).

In contrast to **6**, compound **7** can be viewed as an analog of benzo[*e*]pyrene. The compound absorbs rather inefficiently and only in the UV part of the spectrum (λ_{max} = 367 nm, ε = 6.6 × 10^3 M^{-1} cm^{-1}, Fig. S97). It shows very broad fluorescence of moderate intensity (Φ = 20 ± 3%), thus it can be concluded that spectral properties of **7** are inferior to those of lucigenin.

Fig. 5 shows that the absorption and emission spectra of **8** are rather similar to those of **6** with the exception of strong bathochromic shift (~5600 cm^{-1}, λ_{max} = 610 nm, ε = 1.2 × 10^4 M^{-1} cm^{-1}, Fig. S98). In fact, dye **8** contains the same core structure as **6**, which is further extended with two π-conjugated rings. Disappointingly, the fluorescence quantum yield of **8** was found to be very low (2% for the nitrate form in demineralized water) but increased in less polar solvents (5–6% in acetonitrile). Although the quantum yield increases by several fold depending on solvent and anion, it remains low compared to common luminescent dyes. The luminescence decay time in demineralized water as nitrate salt is τ = 1.3 ± 0.1 ns (Fig. S103).

Fig. 6 shows that fluorescence of **6** and **7** is efficiently quenched by chloride. The Stern–Volmer constants are 160 ± 0.3 M^{-1} (Fig. S79) and 128 ± 0.7 M^{-1} (Fig. S84), respectively, which is about 2-fold and 3-fold lower than for lucigenin ($K_{SV\,NaCl}$ = 360 ± 3 M^{-1}, Fig. S64). In contrast, compound **8** shows only a very weak fluorescence response to chloride ($K_{SV\,NaCl}$ = 4.8 ± 0.1 M^{-1}, Fig. S89) although it is fairly sensitive to heavier halides ($K_{SV\,NaBr}$ = 45.2 ± 0.7 M^{-1}, $K_{stat\,NaBr}$ = 9.7 ± 0.6 M^{-1} (Fig. S90), $K_{SV\,NaI}$ = 63 ± 2 M^{-1}, $K_{stat\,NaI}$ = 9.7 ± 0.6 M^{-1} (Fig. S91)). In comparison, for **6** there is much less difference between its response to chloride and to heavier halides ($K_{SV\,NaBr}$ = 167 ± 0.7 M^{-1}, $K_{stat\,NaBr}$ = 10.5 ± 0.9 M^{-1} (Fig. S80), $K_{SV\,NaI}$ = 122 ± 11 M^{-1}, $K_{stat\,NaI}$ = 39 ± 6 M^{-1} (Fig. S81)). In **7**, the dynamic response towards bromide is higher than for chloride with a marginal contribution of static quenching, whereas iodide shows

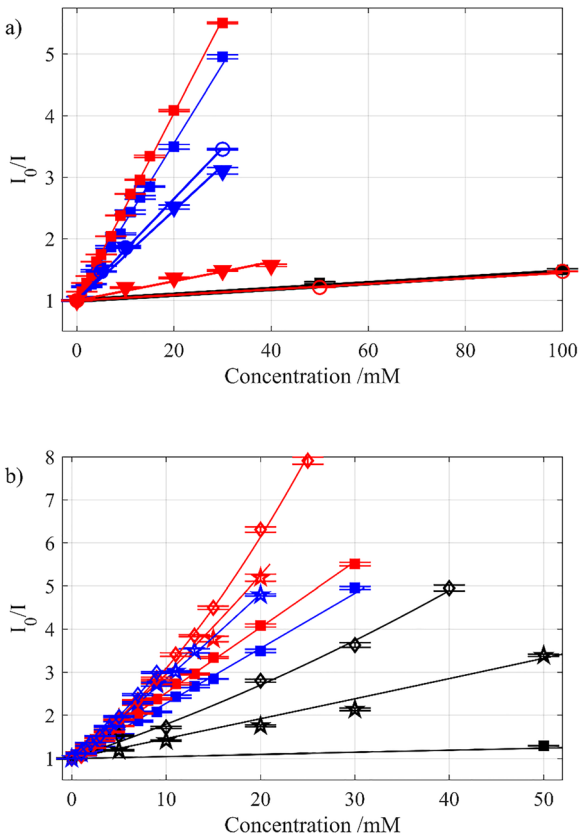

Fig. 6 Fluorescence response of **6** (red), **7** (blue), **8** (black) (all in nitrate forms) dissolved in demineralized water. (a) Response to NaCl (filled square), $NaNO_3$ (hollow circle) and Na_2SO_4 (filled triangle). The data for **8**, which shows virtually no response to $NaNO_3$, are shown in Fig. S88 of the SI. (b) Response to NaBr (hollow star) and NaI (hollow diamond).

very high static contributions ($K_{SV\,NaBr}$ = 175 ± 2 M^{-1}, $K_{stat\,NaBr}$ = 3.7 ± 0.6 M^{-1} (Fig. S85), $K_{SV\,NaI}$ = 81 ± 0.4 M^{-1}, $K_{stat\,NaI}$ = 81 ± 0.4 M^{-1} (Fig. S86)). In both **6** and **7**, the dynamic quenching is stronger for bromide than for iodide, but the static quenching contribution for iodide significantly exceeds that for bromide. For both dyes, the contribution of the static quenching by iodide is much stronger than for the other dyes reported herein, contributing to ~25% of the total quenching for **6** and to ~50% for **7**.

A possible reason for the poor sensitivity of **8** to chloride is the increase in π-electron density hindering the formation of the respective charge-transfer complex with chloride. The effect is essentially the same as for the fluorenyl-extended dye **4**. Thus, it appears that π-extension of the lucigenin structure towards red-shifted chloride-sensitive dyes is very challenging. From literature data[3,13–16] and data herein, it can be seen that chloride sensitivity is a delicate property, which can disappear almost entirely after minor structural changes. However, the example of **6** demonstrates that polycyclic aromatic hydrocarbons can be rendered chloride-sensitive *via* modification with positively-charged nitrogen providing that the π-system is small enough. As can be seen from the comparison of isomers **7** and **6**, the location of absorption and emission bands strongly depends on the 2-dimensional structure of the π-system.

From Fig. 6 we further note that **6** and **8** show relatively low crosstalk to sodium nitrate ($K_{SV\,NaNO_3}$ = 4.5 ± 0.1 M^{-1} (Fig. S78) and 0 M^{-1} (Fig. S88), respectively) and sodium sulphate (15.6 ± 0.2 M^{-1} (Fig. S77) and 6.2 ± 0.3 M^{-1} (Fig. S87), respectively). In contrast, **7** shows enormous crosstalk to the investigated salts ($K_{SV\,Na_2SO_4}$ = 72.6 ± 0.4 M^{-1} (Fig. S82), $K_{SV\,NaNO_3}$ = 82.6 ± 0.1 M^{-1} (Fig. S83)) which further disregards it as a potential chloride indicator.

The halide sensing properties as well as advantages and disadvantages of the compounds investigated are summarized in Table 1. It can be concluded that among all the compounds investigated, **5** and **6** are most promising for chloride-sensing applications showing several attractive characteristics compared to lucigenin. For both dyes, the fluorescence quenching by chloride is roughly half as efficient as for lucigenin.

3.4. Sensor materials

Although **5** in dissolved form may become a viable probe for imaging of chloride with the FLIM technique, many other

Table 1 Summary of halide-sensing properties of investigated compounds

Compound	$K_{SV\,NaCl}$, M^{-1}	$K_{SV\,NaBr}$ ($K_{stat\,NaBr}$) M^{-1}	$K_{SV\,NaI}$ ($K_{stat\,NaI}$) M^{-1}	$K_{SV\,Na_2SO_4}$, M^{-1}	$K_{SV\,NaNO_3}$, M^{-1}	Remarks
1, **2**, **3**	—	—	—	—	—	Not emissive, unsuitable for sensing applications
4	0.8 ± 0	125 ± 6 (8 ± 2)	244 ± 21 (41 ± 10)	0.2 ± 0	0.2 ± 0	Characterized as a product mixture; slightly bathochromically shifted spectra compared to lucigenin
5	145 ± 3	558 ± 2 (2.6 ± 0.3)	656 ± 17 (21 ± 2)	0	0	Spectral properties and brightness virtually identical to lucigenin and much better than for SPQ probe; no cross-talk to nitrate and sulphate; very long fluorescence decay time dependent on chloride concentration
6	160 ± 0.3	167 ± 0.7 (10.5 ± 0.9)	122 ± 11 (39 ± 6)	15.6 ± 0.2	4.5 ± 0.1	Much higher brightness compared to lucigenin, due to higher molar absorption coefficients in the visible part and higher fluorescence quantum yields
7	128 ± 0.7	175 ± 2 (3.7 ± 0.6)	81.1 ± 0.4 (81.1 ± 0.4)	72.6 ± 0.4	82.6 ± 0.1	Poor spectral characteristics, enormous cross-talk
8	4.8 ± 0.1	45.2 ± 0.7 (9.7 ± 0.6)	63 ± 2 (9.7 ± 0.6)	6.2 ± 0.3	0	Very long absorption and emission wavelengths but poor brightness

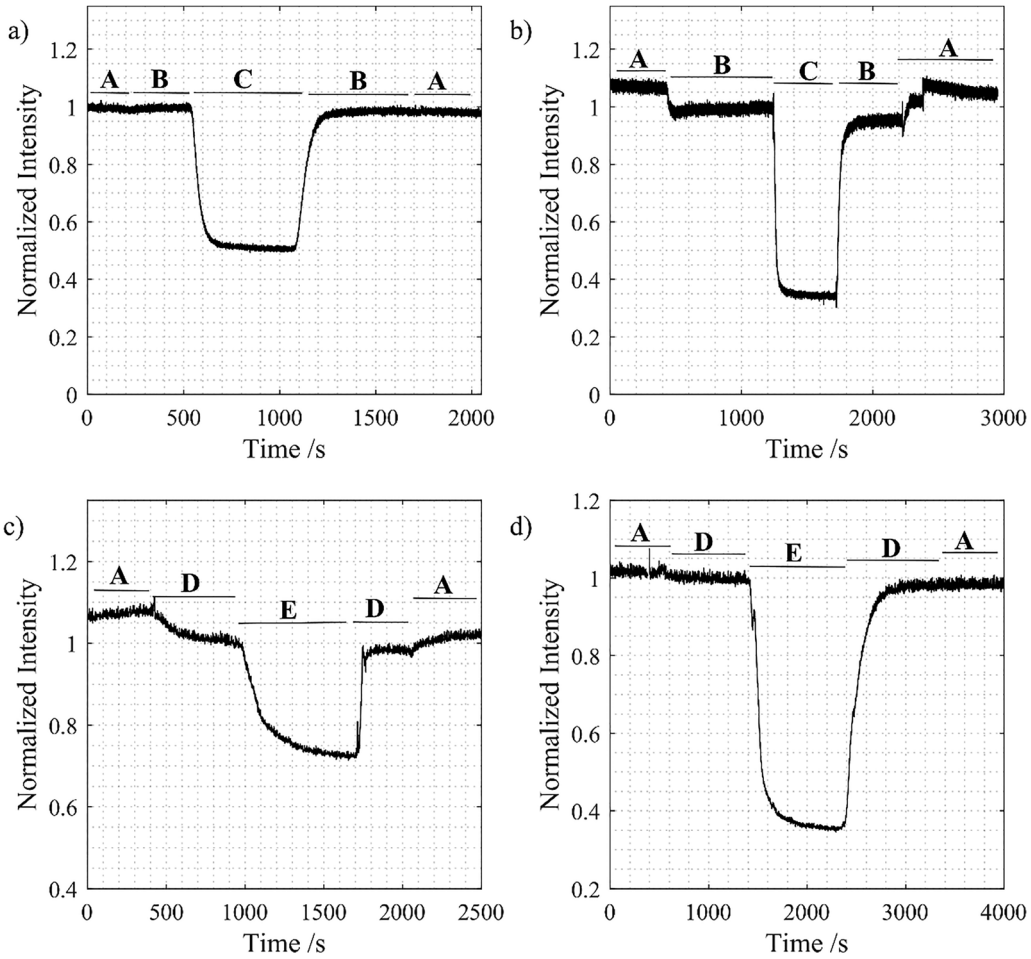

Fig. 7 Response of the sensor materials to chloride and salts ((A) demineralized water, (B) 50 mM $NaNO_3$, (C) 50 mM NaCl, (D) 670 mM Na_2SO_4, (E) 2 M NaCl). (a) and (b) **5** and lucigenin, respectively, photoimmobilized into HYPAN, λ_{exc} = 420 nm, λ_{em} = 500 nm in both cases; (c) **6** immobilized into Nafion membrane, λ_{exc} = 455 nm, λ_{em} = 492 nm; (d) lucigenin immobilized into Nafion membrane, λ_{exc} = 420 nm, λ_{em} = 500 nm.

applications require sensor materials that are prepared upon immobilization of indicators into appropriate polymers. Among others, both hydrolyzed PAN (which is essentially a copolymer of acrylamide and acrylonitrile) and Nafion 117 were reported for immobilization of lucigenin.[11,12] The hydrolyzed PAN (HYPAN) polymer allows for efficient diffusion of ions and thus high efficiency of luminescence quenching by chloride, but the immobilization procedure involves ultraviolet radiation with the immobilization mechanism not clarified. Thus, it cannot be well predicted if a given dye might be efficiently immobilized into the HYPAN polymer or not. On the other hand, positively-charged compounds can be conveniently immobilized into negatively-charged Nafion 117 membrane through electrostatic interactions. However, the negative charges in Nafion 117 lead to a strongly decreased chloride response, rendering the resulting materials more useful for applications in highly saline environments, such as seawater[11] rather than for measurements at physiological conditions.

The photoimmobilisation into HYPAN was explored for **5** and **6**, but unfortunately, **6** could not be immobilized under the same conditions as lucigenin and leached out continuously over time, without reaching a plateau value. In contrast, **5** could be embedded analogously to lucigenin. Fig. 7 shows that the resulting material responds to chloride similarly to HYPAN-immobilized lucigenin. Compound **5** in HYPAN, evidently, does not show noticeable crosstalk to nitrate (Fig. 7a), which is not the case for lucigenin in HYPAN (Fig. 7b).

Since photoimmobilization of **6** into HYPAN was not successful this dye was embedded into the Nafion-117 membrane. Comparison with Nafion-immobilized lucigenin reveals that the latter shows stronger response to chloride and virtually no crosstalk to sulfate (which was selected due to its presence in seawater). Although **6** in Nafion shows chloride response, it may not be sufficient to achieve optimal resolution in seawater (concentration of ~550 mM chloride). It can be concluded that for this dye extended investigation of potentially suitable polymers and immobilization methods remains of considerable interest. For this, chemical modification of the indicator may represent a possible solution. For instance, methyl groups may be substituted with long hydrophobic chains that would allow immobilization into a variety of neutral hydrogel matrices such as poly(2-hydroxyethylmethacrylate) or polyurethane hydrogels.

4. Conclusions

The goal of this study was the preparation and investigation of lucigenin analogs, which show bathochromic shifts of absorption and emission bands compared to this state-of-the-art chloride indicators. The most obvious dyes **1**, **2** and **3**, that all incorporate a benzo[*b*]acridinium part, were found to be non-emissive. A π-extended dye **4**, that incorporates the fluorene backbone, showed desired spectral properties but virtually no response to chloride and no efficient purification method could be found to separate the compound from the by-product. Strong decrease of chloride sensitivity upon π-extension was also observed for dye **8**, a π-extended analog of compound **6**, although it was found sensitive to heavier halides. We therefore suggest that the ratio of quarternized nitrogen atoms to the size of the conjugated system may be a useful indicator whether chloride response is expected or not. The position of the quarternized nitrogen atoms appears to be important as well, as demonstrated for dye **7** that appears to lack chloride sensitivity. The quarternized nitrogen atoms positioned in relatively short proximity might be less efficient in inducing chloride sensitivity.

Among the investigated compounds two promising candidates could be identified. The planar dye **6** can be viewed as an analog of perylene and was found to share its main photophysical characteristics such as position and shape of the absorption and emission bands, Stokes shift and exceptional quantum yield. Being chloride-sensitive, it represents significant improvement over lucigenin in terms of fluorescence brightness. On the other hand, similar to lucigenin, it shows a crosstalk to other ions. The acridinium–quinolinium hybrid **5** and lucigenin show virtually identical spectral properties and comparable brightness, but **5** does not show a crosstalk to nitrate and sulfate in the relevant range. It therefore may be interesting as (i) a water-soluble chloride probe, particularly for imaging using FLIM technique since it also shows remarkably long chloride-dependent fluorescence lifetime, and (ii) in immobilized form, as demonstrated for material prepared on the basis of hydrolyzed PAN. Since immobilization of **6** was only partially successful, further effort can be directed to chemical modification of the dye and its immobilization in different matrices (hydrogels) to fully reveal its full potential as a very bright chloride indicator.

Author contributions

KLS: conceptualization, methodology, investigation, visualization, writing – original draft, writing – review & editing. TM: supervision, writing – review & editing. SMB: conceptualization, writing – review & editing.

Conflicts of interest

There arises no conflict of interests by publishing this work.

Data availability

The data supporting this article have been included as part of the SI. Supplementary information: Overview of the reported acridinium and quinolinium chloride probes; synthetic procedures; nuclear magnetic resonance and mass spectrometry spectra of the dyes and intermediates; absorption and fluorescence spectra, fluorescence decays and Stern–Volmer plots of the investigated compounds. See DOI: **https://doi.org/10.1039/d5tc02192h**.

Acknowledgements

The authors gratefully acknowledge the funding by the Austrian Research Promotion Agency FFG (LumAConM Project-No. 879008), the Austrian Society for Construction Technology ÖBV and the industry partners. Further, we are grateful to Professor Hansjörg Weber from Graz University of Technology for advice and support on nuclear magnetic resonance (NMR) data interpretation.

References

1 K. D. Legg and D. M. Hercules, *J. Phys. Chem.*, 1970, **74**, 2114–2118.
2 F. Wissing and J. A. Smith, *J. Membr. Biol.*, 2000, **177**, 199–208.
3 J. Biwersi, B. Tulk and A. S. Verkman, *Anal. Biochem.*, 1994, **219**, 139–143.
4 S. Jayaraman and A. S. Verkman, *Biophys. Chem.*, 2000, **85**, 49–57.
5 H. Decker and G. Dunant, *Ber. Dtsch. Chem. Ges.*, 1906, **39**, 2720–2722.
6 K. van Dyke, C. van Dyke and K. Woodfork, *Luminescence Biotechnology*, CRC Press, 2001.
7 D. Wöhrle, M. Tausch and W.-D. Stohrer, *Photochemie. Konzepte, Methoden, Experimente*, Wiley-VCH, Weinheim, 1998.
8 I. Stibor, *Anion Sensing*, Springer Berlin, 2014.
9 J. R. Lakowicz, *Principles of Fluorescence Spectroscopy*, Springer US, Boston, MA, 2006.
10 C. Huber, I. Klimant, C. Krause and O. S. Wolfbeis, *Anal. Chem.*, 2001, **73**, 2097–2103.
11 C. Huber, I. Klimant, C. Krause, T. Werner, T. Mayr and O. S. Wolfbeis, *Fresenius' J. Anal. Chem.*, 2000, **368**, 196–202.
12 K. L. Sterz, B. Müller, M. Sakoparnig, I. Galan, A. Steinegger, C. Grengg, F. Mittermayr, S. M. Borisov and T. Mayr, *Talanta*, 2025, **293**, 128124.
13 A. S. Verkman, *Am. J. Physiol.*, 1990, **259**, C375–C88.
14 A. S. Verkman, M. C. Sellers, A. C. Chao, T. Leung and R. Ketcham, *Anal. Biochem.*, 1989, **178**, 355–361.
15 C. Huber, K. Fähnrich, C. Krause and T. Werner, *J. Photochem. Photobiol., A*, 1999, **128**, 111–120.
16 R. Krapf, N. P. Illsley, H. C. Tseng and A. S. Verkman, *Anal. Biochem.*, 1988, **169**, 142–150.
17 N. P. Illsley and A. S. Verkman, *Biochemistry*, 1987, **26**, 1215–1219.

18 N. Chub, G. Z. Mentis and M. J. O'donovan, *J. Neurophysiol.*, 2006, **95**, 323–330.
19 A. C. Engblom and K. E. Akerman, *Biochem. Biophys. Acta*, 1993, **1153**, 262–266.
20 T. Asakawa, H. Kitano, A. Ohta and S. Miyagishi, *J. Colloid Interface Sci.*, 2001, **242**, 284–287.
21 A. J. Pope and R. A. Leigh, *Planta*, 1990, **181**, 406–413.
22 T. Nakamura, H. Kaneko and N. Nishida, *Neurosci. Lett.*, 1997, **237**, 5–8.
23 L. Baù, F. Selvestrel, M. Arduini, I. Zamparo, C. Lodovichi and F. Mancin, *Org. Lett.*, 2012, **14**, 2984–2987.
24 E. Wöll, M. Gschwentner, J. Fürst, S. Hofer, G. Buemberger, A. Jungwirth, J. Frick, P. Deetjen and M. Paulmichl, *Pflugers Archiv*, 1996, **432**, 486–493.
25 C. D. Geddes, K. Apperson, J. Karolin and D. J. Birch, *Anal. Biochem.*, 2001, **293**, 60–66.
26 I. J. Bazany-Rodríguez, D. Martínez-Otero, J. Barroso-Flores, A. K. Yatsimirsky and A. Dorazco-González, *Sens. Actuators, B*, 2015, **221**, 1348–1355.
27 A. Dorazco-González, H. Höpfl, F. Medrano and A. K. Yatsimirsky, *J. Org. Chem.*, 2010, **75**, 2259–2273.
28 F. Zhang, C. Ma, Y. Wang, W. Liu, X. Liu and H. Zhang, *Spectrochim. Acta, Part A*, 2018, **205**, 428–434.
29 A. Dorazco-Gonzalez, *Organometallics*, 2014, **33**, 868–875.
30 R. Salto, M. D. Giron, V. Puente-Muñoz, J. D. Vilchez, L. Espinar-Barranco, J. Valverde-Pozo, D. Arosio and J. M. Paredes, *ACS Sens.*, 2021, **6**, 2563–2573.
31 O. Markova, M. Mukhtarov, E. Real, Y. Jacob and P. Bregestovski, *J. Neurosci. Methods*, 2008, **170**, 67–76.
32 L. J. Galietta, P. M. Haggie and A. S. Verkman, *FEBS Lett.*, 2001, **499**, 220–224.
33 P. Friedel, P. Bregestovski and I. Medina, *Front. Mol. Neurosci.*, 2013, **6**, 7.
34 M. J. Ruedas-Rama, A. Orte, E. A. H. Hall, J. M. Alvarez-Pez and E. M. Talavera, *Analyst*, 2012, **137**, 1500–1508.
35 A. Graefe, S. E. Stanca, S. Nietzsche, L. Kubicova, R. Beckert, C. Biskup and G. J. Mohr, *Anal. Chem.*, 2008, **80**, 6526–6531.
36 R. G. Amiet, *J. Chem. Educ.*, 1982, **59**, 163.
37 J. A. Schneider and D. F. Perepichka, *J. Mater. Chem. C*, 2016, **4**, 7269–7276.
38 C. Qiu and G. J. Blanchard, *J. Phys. Chem. B*, 2014, **118**, 10525–10533.

